

Synthesis and Characterization of ZnO Nanowire–CdO Composite Nanostructures

Karuppanan Senthil · Youngjo Tak ·
Minsu Seol · Kijung Yong

Received: 1 June 2009 / Accepted: 17 July 2009 / Published online: 30 July 2009
© to the authors 2009

Abstract ZnO nanowire–CdO composite nanostructures were fabricated by a simple two-step process involving ammonia solution method and thermal evaporation. First, ZnO nanowires (NWs) were grown on Si substrate by aqueous ammonia solution method and then CdO was deposited on these ZnO NWs by thermal evaporation of cadmium chloride powder. The surface morphology and structure of the synthesized composite structures were analyzed by scanning electron microscopy, X-ray diffraction and transmission electron microscopy. The optical absorbance spectrum showed that ZnO NW–CdO composites can absorb light up to 550 nm. The photoluminescence spectrum of the composite structure does not show any CdO-related emission peak and also there was no band gap modification of ZnO due to CdO. The photocurrent measurements showed that ZnO NW–CdO composite structures have better photocurrent when compared with the bare ZnO NWs.

Keywords Zinc oxide · Cadmium oxide · Nanowires · Composites · Optical absorbance

Introduction

Zinc oxide (ZnO) is one of the most important materials for the optoelectronic applications because of its wide band gap (3.37 eV) and high-exciton binding energy (60 meV) that is much larger than other semiconductor materials such as ZnSe (22 meV) and GaN (25 meV). ZnO nanostructures have been extensively investigated in the past decade due to their interesting optical [1, 2] and electrical properties [3–6]. These nanostructures have potential applications as UV light sources, photodetectors, sensors, photocatalysts, solar cells, field effect transistors, field emission devices and piezoelectric devices [5–12]. Among the various ZnO nanostructures, ZnO nanowires have attracted much attention because of their unique material properties and well-developed synthesis methods. Various methods have been employed to fabricate ZnO nanowires including gas-phase methods such as metal-organic chemical vapor deposition (MOCVD) [13], evaporation [14], pulsed-laser deposition [15], solution-phase methods such as chemical bath deposition (CBD) [16], electrochemical deposition [17] and hydro-thermal method [18]. Especially, solution-phase methods are appealing because of the low growth temperatures, potentials for scaling up and capability of producing high-density arrays [19].

Recently, ZnO nanowire arrays have been applied as a transparent electrode in the solar energy devices due to their high surface area and good vertically aligned electrical pathways, which are expected to increase the efficiency of these photoelectric devices [11, 20, 21]. However, ZnO can only absorb a small portion of the solar spectrum in the visible region due to its wide band gap. To further widen the useable wavelength range and improve the efficiency of ZnO-based photodevices, a narrow band gap material should be alloyed or composited with ZnO. In principle, the

K. Senthil
Center for Information Materials, Pohang University of Science and Technology (POSTECH), San 31, Hyoja-dong, Nam-gu, Pohang 790-784, South Korea

Y. Tak · M. Seol · K. Yong (✉)
Department of Chemical Engineering, Pohang University of Science and Technology (POSTECH), San 31, Hyoja-dong, Nam-gu, Pohang 790-784, South Korea
e-mail: kyong@postech.ac.kr

coupling of ZnO with a narrow band gap material, can reduce its band gap, extend its absorption range to visible-light region, promote electron-hole pair separation under irradiation and consequently achieve a higher efficiency for the ZnO-based photodevices. In recent years, heterostructures of ZnO with metals or semiconductors have attracted much attention because of their enhanced optical and photocatalytic properties [22–30].

CdO, an *n*-type II–VI semiconductor, has attracted considerable attention for various optoelectronic devices due to its high electrical conductivity (even without doping), high carrier concentration and high optical transmittance in the visible region of the solar spectrum. By alloying with CdO, which has a cubic structure and a narrower direct band gap of 2.2–2.5 eV, the band gap of ZnO can be red-shifted to a blue or even a green spectral range. Wang et al. [31] have shown that UV near-band-edge emission was red-shifted to 407 nm (3.04 eV) from 386 nm (3.21 eV) with the increasing Cd content for their quasi-aligned ZnCdO nanorods. Up to our knowledge, there are no reports available on the heterostructures of ZnO nanostructures with CdO. In the present study, we report the synthesis and characterization of ZnO nanowire–CdO composite structures by a two-step process involving chemical solution method and thermal evaporation. The synthesized ZnO NW–CdO composite structures showed enhanced optical absorbance in the visible region.

Experiment

ZnO NW–CdO composite structures were fabricated on silicon substrates by using a two-step process. First, ZnO NWs were grown on Si substrates using the previously reported ammonia solution method [32, 33]. A 25 nm ZnO buffer film was coated on the Si substrate by sputtering a ZnO target at room temperature and then was air-annealed at 800 °C for 1 h. After cooling to room temperature, the substrates were immersed in a 10 mM $\text{Zn}(\text{NO}_3)_2 \cdot 6\text{H}_2\text{O}$ (98%, Aldrich) aqueous solution where pH was adjusted to 11 by adding the ammonia solution [28 wt% of NH_3 (Aldrich) in water], and the solution was heated at 95 °C for 10 h. After the growth, the substrate was removed from the solution, rinsed with the deionized water and then dried by nitrogen blow. Then ZnO NW–CdO composite structures were grown by thermal evaporation of CdCl_2 powder in argon atmosphere using a conventional horizontal tube furnace. Pure CdCl_2 powder was deposited in the middle of the alumina boat and the ZnO NW substrate was placed on the top of the boat with the ZnO nanowire surface facing the powder. The alumina boat was then placed at the uniform-temperature zone of the furnace and heated to 500–550 °C (ramp rate ~ 12 °C/min) with a constant argon

flow of 100 sccm. The temperature was maintained at 500–550 °C for about 1 h and then the furnace was allowed to cool normally to room temperature before taking the sample out for characterization. When CdCl_2 is evaporated, CdO is formed on ZnO NWs by taking the residual oxygen present in the furnace.

The surface morphology, structure and composition of the as-grown ZnO NW and ZnO NW–CdO composites were characterized by field emission scanning electron microscopy (FE-SEM; JEOL JSM 330F), X-ray diffraction (XRD; Rigaku D-Max1400, Cu $K\alpha$ radiation $\lambda = 1.5406$ Å), Raman spectroscopy (SENTERRA dispersive Raman microscope, 532 nm laser wavelength), high-resolution transmission electron microscopy (HR-TEM; JEOL 2100F) and energy-dispersive X-ray spectroscopy (EDX) measurements. The optical absorbance (diffuse reflectance spectroscopy—DRS) measurements were carried out using a UV-visible spectrophotometer. The photoluminescence measurements were carried out at room temperature using He–Cd laser (325 nm) as the excitation source. The photocurrent measurements were carried out in a typical three-electrode cell (Potentiostat/Galvanostat, Model 263A) that included a Pt counter electrode, a saturated calomel reference electrode and a working electrode made from ZnO NW or ZnO NW–CdO composites on the ITO substrate. A 1 M Na_2S solution was used as the electrolyte. The working electrode was illuminated from front side with a solar-stimulated light source (AM1.5G filtered, 100 mW/cm², 91160, Oriel).

Results and Discussion

Figure 1a, b shows the low and high magnification cross-sectional FE-SEM images of ZnO NW array grown on Si substrate. The grown nanowire array was highly dense and vertically well aligned. The nanowires were about 50–100 nm in diameter and 4–5 μm in length. CdCl_2 powder (0.4 and 0.6 g) was evaporated on these nanowire arrays to obtain ZnO NW–CdO composite structures. Figure 1c–f shows SEM images of the ZnO NW–CdO composite structures grown using 0.4 and 0.6 g of CdCl_2 powder, respectively. It can be seen that the surface of the ZnO NW becomes rough and CdO layer was found deposited mainly on the tip of the ZnO nanowires. With the increase of CdCl_2 powder, the amount of CdO deposited on the tips increased.

X-ray diffraction patterns obtained from the as-grown ZnO NWs and ZnO NW–CdO composite structure were shown in Fig. 2a, b, respectively. As-grown ZnO NW sample showed major XRD peaks at 2θ of 34.54° and 62.98° that can be indexed to reflections from (002) and (103) planes of hexagonal ZnO, respectively, according to

Fig. 1 SEM images (cross-sectional and tilted view) obtained from **a, b** ZnO NWs; **c, d** ZnO NW–CdO composites (0.4 g of CdCl₂) and **e, f** ZnO NW–CdO composites (0.6 g of CdCl₂)

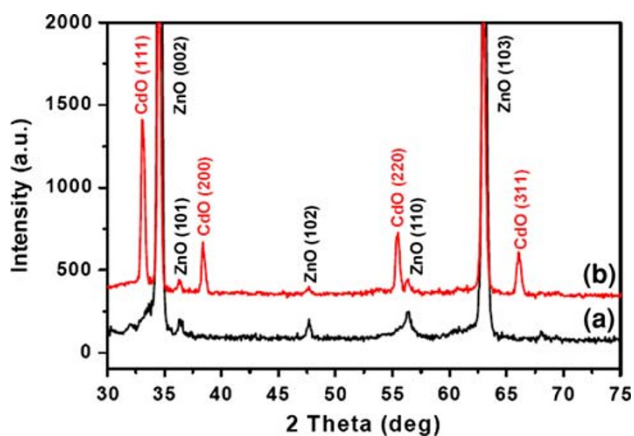
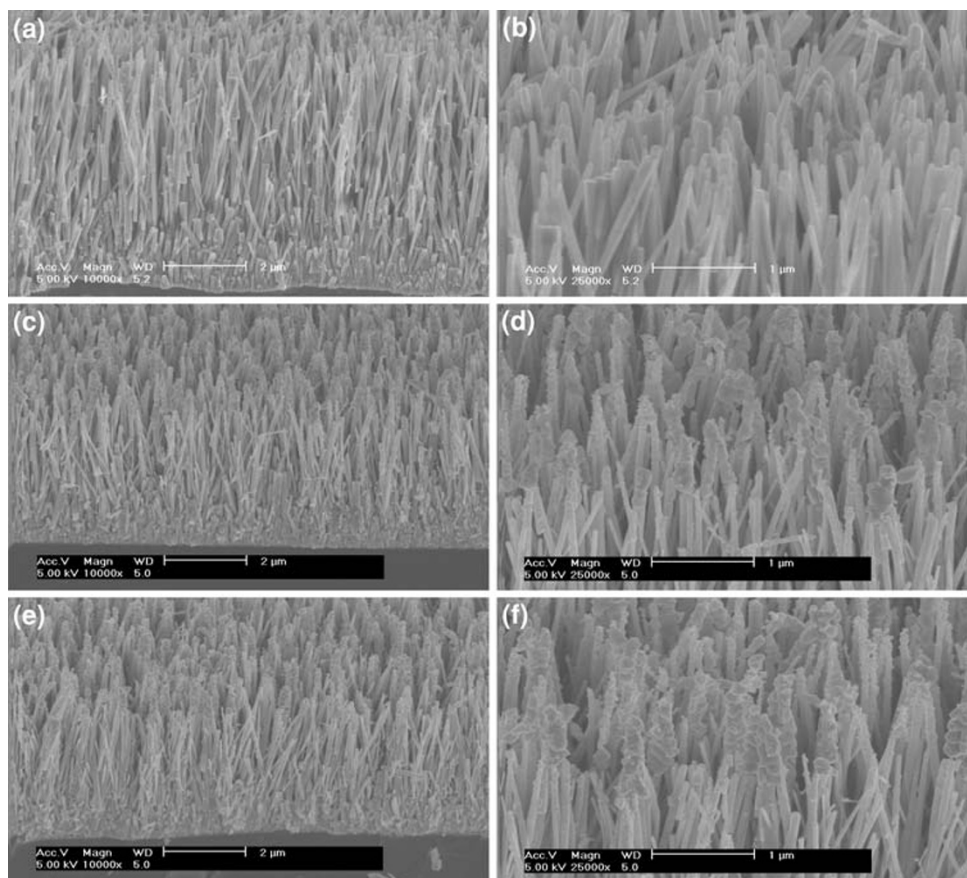


Fig. 2 X-ray diffraction pattern obtained from the **a** ZnO NWs and **b** ZnO NW–CdO composites

JCPDS no. 36-1451. The peaks from (101), (102) and (110) planes of ZnO were also observed. XRD pattern obtained from the ZnO NW–CdO composite structure showed additional peaks from (111), (200), (220) and (311) planes corresponding to cubic CdO (JCPDS no. 05-0640) beside hexagonal ZnO peaks. The ZnO-related XRD peaks observed for the ZnO NW–CdO composite structure were slightly deviated from the peaks observed for the ZnO NW

sample. This suggests that there might be a very small ZnCdO phase at the interface.

Figure 3 shows the Raman spectrum obtained from the as-grown ZnO NW and ZnO NW–CdO composite structure. The Raman spectrum from the as-grown ZnO NW sample (Fig. 3a) exhibited E₂ (high) and A₁ (LO) modes at 437 and 581 cm⁻¹, respectively. The Raman spectrum was recorded with the incident light exactly perpendicular to the top of the sample surface (the incident light is parallel to the *c*-axis of the ZnO NWs). In this configuration, only the E₂ and A₁ (LO) modes are allowed, whereas the A₁(TO) and E₁(TO) modes are forbidden according to the Raman selection rules. The presence of LO modes and the absence TO modes in the Raman spectrum further confirms that the grown nanowires are vertically aligned with *c*-axis oriented. The peak at 275 cm⁻¹ could be attributed to the B₁ (low) silent Raman mode [34]. The Raman spectrum from the ZnO NW–CdO composite structure (Fig. 3b) is similar like ZnO NW sample and showed Raman peaks only from ZnO and do not show any CdO-related Raman peak. The assignment of Raman mode of CdO is very difficult and it is known that mostly CdO is Raman inactive [35]. This could be attributed to the absence of CdO-related Raman peak for our composite structures. A slight shift in E₂ (high) Raman mode was

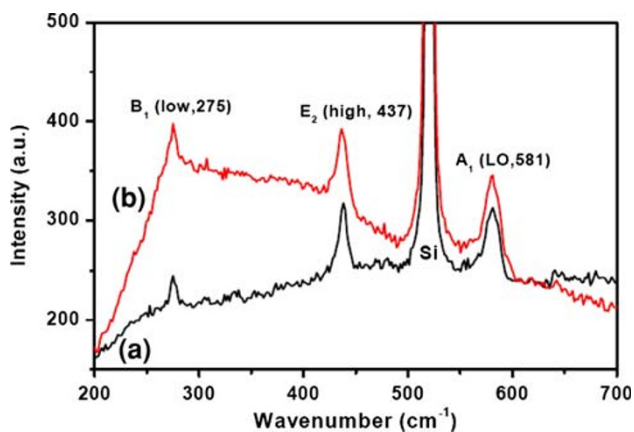


Fig. 3 Raman spectra of **a** ZnO NWs and **b** ZnO NW-CdO composites

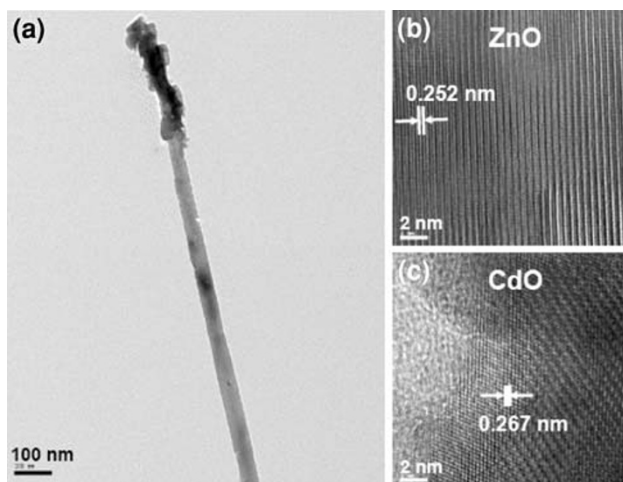


Fig. 4 **a** TEM image obtained from the ZnO NW-CdO composite and **b**, **c** HRTEM lattice images obtained from the ZnO and CdO regions, respectively

reported for the case of ZnCdO nanorods [36]. In our case, we could not observe any shift in that Raman mode because the obtained nanostructures are ZnO NW-CdO composite structure.

The detailed microscopic structure and chemical composition of the ZnO NW-CdO composite structures were analyzed by using a high-resolution scanning transmission electron microscope (HR-STEM). Figure 4a shows the low magnification TEM image of the ZnO NW-CdO composite structure showing a single ZnO nanowire with CdO layer coated only on the upper part of the nanowire up to a certain length (a few hundreds nm) from the tip. It was observed that the CdO-coated surface was rougher than that of the bare ZnO NW surface. Figure 4b, c shows the HR-TEM lattice images from the ZnO and CdO regions of ZnO NW-CdO composite structure, respectively. There

might be a very small ZnCdO phase at the interface. But we could not identify the ZnCdO phase clearly from the HR-TEM analysis. The lattice image from the ZnO NW showed clear lattice fringes confirming the single crystalline ZnO. The measured lattice spacing of the crystallographic plane is 0.252 nm, which corresponds well with the (002) plane (0.25 nm) of hexagonal ZnO. The lattice spacing measured from the CdO lattice image is 0.267 nm and this value corresponds well with the *d*-value (0.271 nm) of (111) plane of cubic CdO. Figure 5a shows TEM image from the ZnO NW-CdO composite structure and Fig. 5b–d shows EDX elemental mapping corresponding to Zn, O and Cd, respectively. The elemental mapping further confirms that CdO is coated only on the tip of the ZnO NWs.

Figure 6 shows the DRS spectra of the as-grown ZnO NWs and ZnO NW-CdO composite structures. Because CdO is a narrow band gap material, it is expected that optical absorbance region will be extended to the visible region for the ZnO NW-CdO composite structures. The optical absorbance edge for the ZnO NWs is found to be about 400 nm, whereas the ZnO NW-CdO composites absorb light up to 550 nm in the visible region. The inset of the Fig. 6 shows the digital photograph images of the ZnO NW and ZnO NW-CdO composite samples. We can observe that the color of the ZnO NW samples changed from gray to yellow-orange color after CdO deposition.

Figure 7 shows the room temperature PL spectra from the ZnO NWs annealed in H₂ atmosphere at 400 °C and ZnO NW-CdO composite structures. The PL spectrum from the ZnO NWs shows an intense UV emission peak at 377 nm without any defect emissions. This result suggests that the grown ZnO NWs have high crystalline quality. The PL spectrum from the ZnO NW-CdO composites showed a UV emission peak at 381 nm, and no emission band from CdO was observed. The UV emission peak is attributed to the near-band-edge exciton emission. It has been reported that the UV emission peak has been red-shifted to 407 nm with increasing Cd content for the case of ZnCdO nanorods indicating a band gap modulation [31]. For our composite nanostructures, the peak position of the near-band-edge emission is slightly red-shifted and also the intensity is reduced when compared with the UV emission peak of the ZnO nanowire. The slight red-shift in the emission peak could be attributed to the existence of ZnCdO phase at the interface. The reduced PL intensity could be attributed to the quenching effects. A similar behavior has been reported for the CdS nanoparticle modified ZnO nanowalls [37]. The rock salt CdO is known to have at least one indirect optical transition with the band gap energy of 0.8 eV below the direct absorption edge at 2.4 eV [38]. The absence of any CdO-related PL peak in our case may be attributed to this indirect nature of the rock salt CdO structure.

Fig. 5 **a** TEM image of the ZnO NW–CdO composite structure showing CdO deposition only on the tip of the ZnO nanowire and their corresponding EDX elemental mapping of **b** Zn, **c** O and **d** Cd, respectively

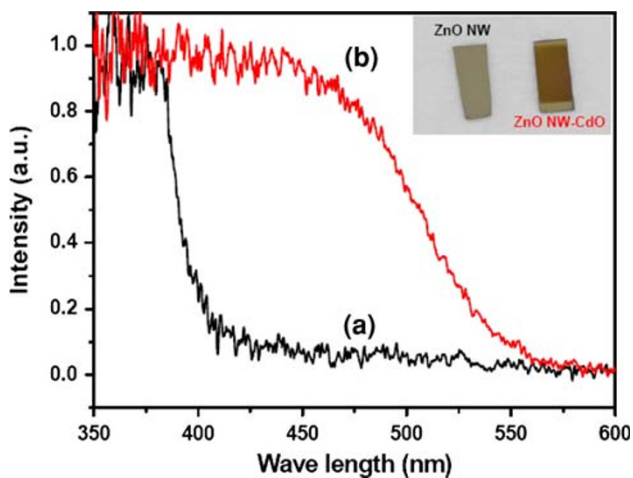
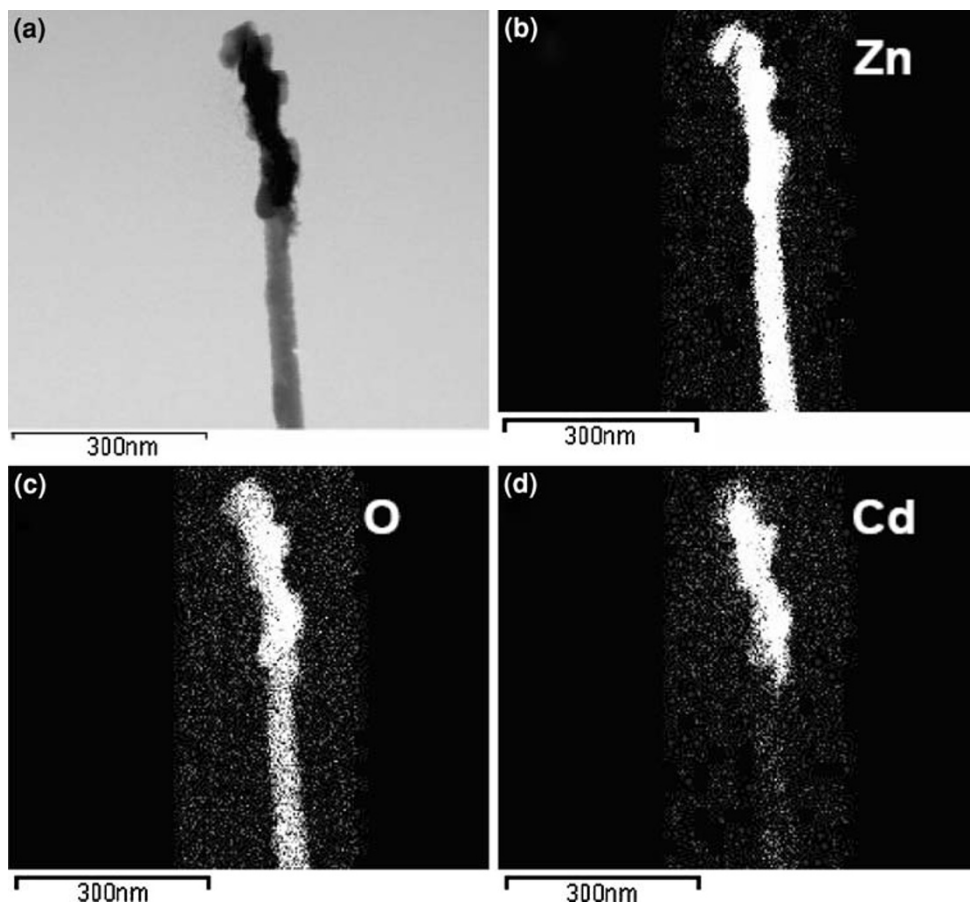


Fig. 6 Diffuse reflectance spectra (*DRS*) of **a** ZnO NWs and **b** ZnO NW–CdO composites. The *inset* shows the digital photograph of the ZnO NW and ZnO NW–CdO composite samples

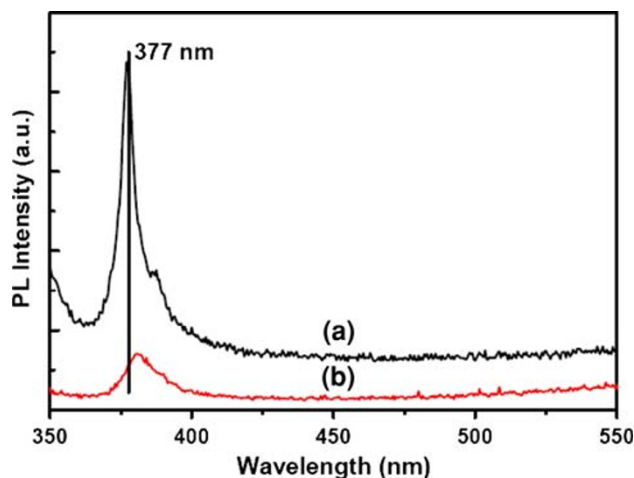


Fig. 7 Room temperature photoluminescence spectra obtained from the **a** ZnO NWs and **b** ZnO NW–CdO composites

Preliminary experiments were carried out using ZnO NW–CdO composites on ITO substrate as the electrode material in the photoelectrochemical cell (PEC). The photoresponse measurements were carried out at 0 V. The dark and photocurrent characteristics (current vs. time) of the

ZnO NWs and ZnO NW–CdO composites measured at 0 V are given in Fig. 8. A higher photocurrent was observed for the ZnO NW–CdO composites when compared with the bare ZnO NWs. The optical absorption capability in the visible region could be attributed to the higher photocurrent for the ZnO NW–CdO composite structures. Systematic

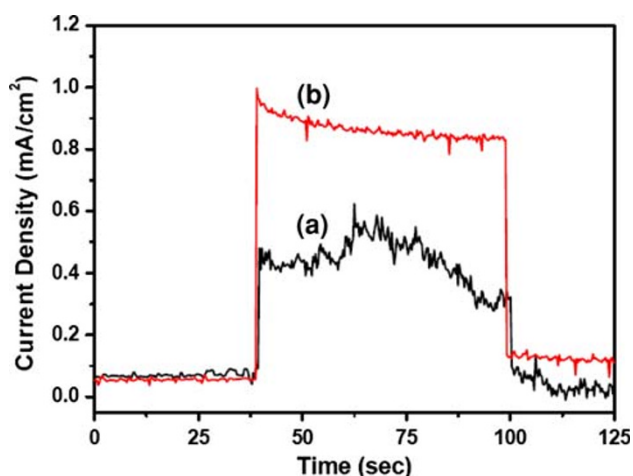


Fig. 8 The photoresponse characteristics of **a** ZnO NWs and **b** ZnO NW–CdO composites

investigations are now in progress to improve the photo-conversion efficiency of these composite structures by optimizing the various parameters such as substrate material (Pt-coated Si or FTO), electrolytes and CdO deposition conditions. The studies on photodegradation of organic dyes are also now in progress to explore the photocatalytic properties of these composite structures.

Conclusions

We synthesized ZnO NW–CdO composite structures using a simple two-step process involving ammonia solution method followed by thermal evaporation. SEM and TEM analysis indicated that CdO was deposited mainly on the tip of the ZnO nanowires. XRD analysis of the composite structures showed additional diffraction peaks corresponding to cubic CdO, apart from the signals from the hexagonal ZnO. The ZnO NW–CdO composite structures showed enhanced optical absorption extending to about 550 nm in the visible region. PL measurements do not show any band gap modification for the composite structures. The higher visible-light absorption capability of these composite structures can be applied to enhance their photoelectrochemical and photocatalytic properties. Systematic studies are now in progress to explore these properties.

Acknowledgments This work was supported by grant no. R01-2006-000-10230-0 (2006) from the Korea Science and Engineering Foundation, grant no. RTI04-01-04 from the Regional Technology Innovation Program of the Ministry of Commerce, Industry and Energy (MOCIE) and the Korean Research Foundation Grants funded by the Korean Government (MOEHRD; KRF-2005-005-J13101) and grant no. KRF-2007-521-D00118.

References

1. A.B. Djurisic, Y.H. Leung, *Small* **2**, 944 (2006)
2. M.H. Huang, S. Mao, H. Feick, H. Yan, Y. Wu, H. Kind, E. Weber, R. Russo, P. Yang, *Science* **292**, 1897 (2001)
3. M.H. Zhao, Z.L. Wang, S. Mao, *Nano Lett.* **4**, 587 (2004)
4. Z.Y. Fan, J.G. Lu, *Appl. Phys. Lett.* **86**, 032111 (2005)
5. X. Wang, J.L.J. Song, Z.L. Wang, *Science* **316**, 102 (2007)
6. C.J. Lee, T.J. Lee, S.C. Lyu, Y. Zhang, H. Ruh, H.J. Lee, *Appl. Phys. Lett.* **81**, 3648 (2002)
7. Z.L. Wang, *J. Phys. Cond. Matt.* **16**, R829 (2006)
8. L. Schmidt-Mende, J.L. MacManus-Driscoll, *Mater. Today* **10**, 40 (2007)
9. N. Kouklin, *Adv. Mater.* **20**, 2190 (2008)
10. Y. Qin, X. Wang, Z.L. Wang, *Nature* **451**, 809 (2008)
11. J.B. Baxter, E.S. Aydil, *Appl. Phys. Lett.* **86**, 053114 (2005)
12. Q. Wan, Q.H. Li, Y.J. Chen, T.H. Wang, X.L. He, J.P. Li, C.L. Lin, *Appl. Phys. Lett.* **84**, 3654 (2004)
13. W.I. Park, G.C. Yi, M. Kim, S.J. Pennycook, *Adv. Mater.* **14**, 1841 (2002)
14. S.Y. Bae, C.W. Na, J.H. Kang, J.G. Park, *J. Phys. Chem. B* **109**, 2526 (2005)
15. Y. Zhang, R.E. Russo, S.S. Mao, *Appl. Phys. Lett.* **87**, 133115 (2005)
16. J. Song, S.J. Lim, *J. Phys. Chem. C* **111**, 596 (2007)
17. J.B. Cui, U.J. Gibson, *J. Phys. Chem. B* **109**, 22074 (2005)
18. C.H. Lu, L.M. Qi, J.H. Yang, L. Tang, D.Y. Zhang, J.M. Ma, *Chem. Comm.* 3551 (2006)
19. L.E. Greene, B.D. Yuhus, M. Law, D. Zitoun, P. Yang, *Inorg. Chem.* **45**, 7535 (2006)
20. C. Levy-Clement, R. Tena-Zaera, M.A. Ryan, A. Katty, G. Hodes, *Adv. Mater.* **17**, 1512 (2005)
21. Y. Gao, M. Nagai, T.C. Chang, J.J. Shyue, *Crys. Growth Des.* **7**, 2467 (2007)
22. W.Q. Zhang, Y. Lu, T.K. Zhang, W.P. Xu, M. Zhang, S.H. Yu, *J. Phys. Chem. C* **112**, 19872 (2008)
23. Y. Zheng, L. Zheng, Y. Zhan, X. Lin, Q. Zheng, K. Wei, *Inorg. Chem.* **46**, 6980 (2007)
24. J. Nayak, S.N. Sahu, J. Kasuya, S. Nozaki, *Appl. Surf. Sci.* **254**, 7215 (2008)
25. Y. Tak, H. Kim, D. Lee, K. Yong, *Chem. Comm.* 4585 (2008)
26. T. Gao, Q.H. Li, T.H. Wang, *Chem. Mater.* **17**, 887 (2005)
27. R. Tena-Zaera, A. Katty, S. Bastide, C. Levy-Clement, *Chem. Mater.* **19**, 1626 (2007)
28. Z. Wang, B. Huang, Y. Dai, X. Qin, X. Zhang, P. Wang, H. Liu, J. Yu, *J. Phys. Chem. C* **113**, 4612 (2009)
29. D. Lin, H. Wu, W. Zhang, H. Li, W. Pan, *Appl. Phys. Lett.* **94**, 172103 (2009)
30. Y. Tak, S.J. Hong, J.S. Lee, K. Yong, *Cryst. Growth Des.* **9**, 2627 (2009)
31. F.Z. Wang, Z.Z. Ye, D.W. Ma, L.P. Zhu, F. Zhuge, H.P. He, *Appl. Phys. Lett.* **87**, 143101 (2005)
32. Y. Tak, K. Yong, *J. Phys. Chem. C* **112**, 74 (2008)
33. Y. Tak, K. Yong, *J. Phys. Chem. B* **109**, 19263 (2005)
34. F.J. Manjon, B. Mari, J. Serrano, A.H. Romera, *J. Appl. Phys.* **97**, 053516 (2005)
35. Z.V. Popovic, G. Stanisc, D. Stojanovic, R. Kostic, *Phys. Stat. Sol.* **165**(b), K109 (1991)
36. F. Wang, H. He, Z. Ye, L. Zhu, H. Tang, Y. Zhang, *J. Phys. D* **38**, 2919 (2005)
37. F. Fang, D.X. Zhao, B.H. Li, Z.Z. Zhang, J.Y. Zhang, D.Z. Shen, *Appl. Phys. Lett.* **93**, 233115 (2008)
38. A.B.M.A. Ashrafi, H. Kumano, I. Suemune, Y.W. Ok, T.Y. Seong, *Appl. Phys. Lett.* **79**, 470 (2001)